Mn$_3$O$_4$ nano-sized crystals: Rapid synthesis and extension to preparation of nanosized LiMn$_2$O$_4$ materials

XIAO-LING CUI, YONG-LI LI, SHI-YOU LI*, GUO-CUN SUN, JIN-XIA MA, LU ZHANG, TIAN-MING LI and RONG-BO MA

College of Petrochemical Technology, Lanzhou University of Technology, Lanzhou 730050, China
e-mail: lishiyoulw@163.com

Abstract.　With a novel gas–liquid reaction, a facile and rapid method has been successfully developed for the synthesis of nano-sized Mn$_3$O$_4$ crystals. Coupled with complementary experiments, preparation mechanisms of Mn(II) and Mn(III)Mn(III)Mn(II) coordination complexes as well as nano-sized Mn$_3$O$_4$ crystals are studied. Besides, as the extension of synthesis of nano-sized Mn$_3$O$_4$ crystals, the intermediate ammonia alkaline solution containing Mn(III)Mn(III)Mn(II) coordination complexes, which tend to decompose into nano-sized Mn$_3$O$_4$ crystals spontaneously, are used to prepare nanosized LiMn$_2$O$_4$ materials. Although any physical treatment has been done to disperse powders, the as-synthesized LiMn$_2$O$_4$ nanoparticles are still existence with homogeneous size distribution (about 24.2 nm) without any obvious agglomeration. That is to say, the novel method is constructive not only to accelerate reaction rates for the elevated oxidation state of manganese ions, but also to prepare dispersed nanosized LiMn$_2$O$_4$ materials with good electrochemical properties.

Keywords.　Lithium batteries; materials preparations; Mn$_3$O$_4$; LiMn$_2$O$_4$; nanoparticles.

1. Introduction

Manganese oxides are important materials in many applications such as magnetic storage media, catalysis, electrodes, ion exchangers, and sensors.[1–3] Particularly, Mn$_3$O$_4$ is known to be an effective and inexpensive catalyst in various oxidation and reduction reactions.[4–6] Nanoscale Mn$_3$O$_4$ materials with large specific surface areas are of great interest for researchers from a broad range of disciplines.[7]

Mn$_3$O$_4$ nanoparticles have been synthesized by a series of methods, as shown in table 1. Overall, the synthesis mechanism of Mn$_3$O$_4$ can be divided into two main categories. The first category is the oxidative pyrolysis of manganese salts, such as the calcination method and the thermal decomposition method.[8,9] These methods are simple and reliable, without filtering, drying and other processes. But each of them takes expensive precursor materials and high energy consumption. The second category is the method for the oxidation of intermediate manganese hydroxide (Mn(OH)$_2$), such as the solvothermal method, the refluxing method, the hydrothermal method, and the self-assembly method.[10–13] These preparation methods are cheap to make, but relatively time consuming,

because of Mn$_3$O$_4$ nanoparticles being synthesized via a gas–solid reaction between O$_2$ and Mn(OH)$_2$.

Due to the fact that gas–liquid reaction method can provide a large surface area to promote the interface reaction, it is generally believed that the formation rate of Mn$_3$O$_4$ nanoparticles would be accelerated dramatically when the gas–solid reaction method is replaced by a gas–liquid reaction method. However, given that the oxidation of Mn(II) occurs under alkaline condition, the gas–liquid reaction is difficult to achieve, because in this case, Mn(II) ions are most likely to be existed as Mn(OH)$_2$ precipitates.

Therefore, the exploring of a novel, low-cost, simple and fast method for preparation of Mn$_3$O$_4$ nanoparticles is of special interest. And in this process, replacing Mn(OH)$_2$ precipitates with free and soluble Mn(II) ions under alkaline condition is the most critical and hardest step.

In this work, we report the preparation of nanosized Mn$_3$O$_4$ crystals by a gas–liquid reaction method, with the relatively cheap raw materials of Mn(CH$_3$COO)$_2$·4H$_2$O and a rapid reaction time of 5 min at 50°C.

Besides, as a typical example of application, the resulting nano-sized Mn$_3$O$_4$ crystals could be used as raw materials for the preparation of nanosized LiMn$_2$O$_4$ materials, based upon considerations as follows. Firstly, LiMn$_2$O$_4$-based materials are promising candidates for

*For correspondence

Table 1. Some details of synthesis methods for Mn_3O_4 nanoparticles.

Synthesis method	Synthesis temperature (°C)	Synthesis time (h)	Precursor materials	Particle size (nm)
Calcination method[8]	800	3	$Mn(CH_3COO)_2 \cdot 4H_2O$, Mn(acetylacetonate)$_3$ and egg white	60
Thermal decomposition method[9]	260	1	Bis(2-hydroxy-1-naphthaldehydato) manganese(II)	9–24
Solvothermal method[10]	160	24	$MnCl_2$, NaOH and 1, 10-phenanthroline	60
Refluxing method[11]	100	4	Manganese hydroxide and gel	50
Hydrothermal method[12]	200	24	$Mn(NO_3)_2$ solution (50 wt%)	26
Self-assembly method[13]	60	24	$KOH–C_2H_5OH$ and $Mn(CH_3COO)_2 \cdot 4H_2O–C_2H_5OH$	4.5

lithium-ion batteries, coupled with their own advantages as well as developments of electric vehicles (EVs) and hybrid electric vehicles (HEVs).[14,15] Secondly, replacing Mn(II) compounds with Mn_3O_4 materials is good for the preparation of $LiMn_2O_4$ materials, due to the fact that the elevated oxidation state of manganese ions could reduce the negative effect for the lack of oxygen, which is detrimental to the oxidation reaction and would lead to consequent damages, such as the Mn dissolution, the structure distortion, and the capacity to fade upon cycling.[16,17] Thirdly, the solution containing the precursor of nano-sized Mn_3O_4 crystals and the preferred lithium source of $LiNO_3$ would form a gel state via evaporation in the reaction process, which would allow precise control of the stoichiometric amount at the micro level. Fourthly, the newly as-synthesized nano-sized Mn_3O_4 crystals would play crucially important roles in the formation of nanosized $LiMn_2O_4$ materials, serving as crystal nucleus to disperse preliminary granules evenly. Lastly, as mentioned above, the obtained $LiMn_2O_4$ precursor is made up of tiny and homogeneous particles, which will contribute to both of the decrease in reaction temperature and restraint on particle agglomeration.

2. Experimental

2.1 *Rapid preparation of nano-sized Mn_3O_4 crystals*

4.9018 g (20 mmol) of $Mn(CH_3COO)_2 \cdot 4H_2O$ was dissolved in 100 mL of ethanol. After the addition of 40 mL of $NH_3 \cdot H_2O$ (25 wt%–28 wt%), the colourless solution was changed to light red, but without any precipitate. Then, 1.5 $L \cdot min^{-1}$ of air was blown into the solution for 5 min at 50°C. And during this process, the solution colour would change gradually to deep black, with consequent decomposition to form a colloidal solution, where particles were dispersed

evenly and stably in the solution. Removing the supernatant after centrifugation, nano-sized Mn_3O_4 crystals would be obtained, named M-1. And hardly any manganese compounds could be detected in the supernatant.

2.2 *Preparation of nanosized $LiMn_2O_4$ materials*

Both 4.9018 g (20 mmol) of $Mn(CH_3COO)_2 \cdot 4H_2O$ and 0.6895 g (10 mmol) of $LiNO_3$ were dissolved in 100 mL of ethanol. After similar processes with the rapid preparation of nano-sized Mn_3O_4 crystals, a black colloidal solution containing nano-sized Mn_3O_4 crystals and the preferred lithium source of $LiNO_3$ would be got. In the course of this preparation, nano-sized Mn_3O_4 crystals and $LiNO_3$ raw materials are dispersed evenly and stable throughout the liquid, which could extremely allow precise control of the stoichiometric amount at the micro level. Then, with the aim of evaporating solvents, the resulting colloidal solution was heated to 80°C under normal stirring conditions. The evaporation stage would be continued until the formation of a black gelatinous precursor. The resulting precursor was fired for 10 h at 650°C, and then the final product of nanosized $LiMn_2O_4$ materials would be obtained.

2.3 *Cell preparation*

The resulting nanosized $LiMn_2O_4$ materials were mixed with carbon black and poly(vinylidene fluoride) at a weight ratio of 84: 8: 8 in N-methyl pyrrolidinone to prepare a sheet electrode.

Experimental cells (CR2032 type, 20 mm in diameter and 3.0 mm in thickness) were assembled in a glove box using the thus prepared sheet electrode as a cathode material, a lithium sheet as an anode material, a typical system consisting of 1.0 $mol \cdot L^{-1}$

LiPF$_6$-ethylene carbonate (EC)/dimethyl carbonate (DMC) (1:1, by volume) as a electrolyte material, and a Celgard (2400) porous polypropylene as a separator material.
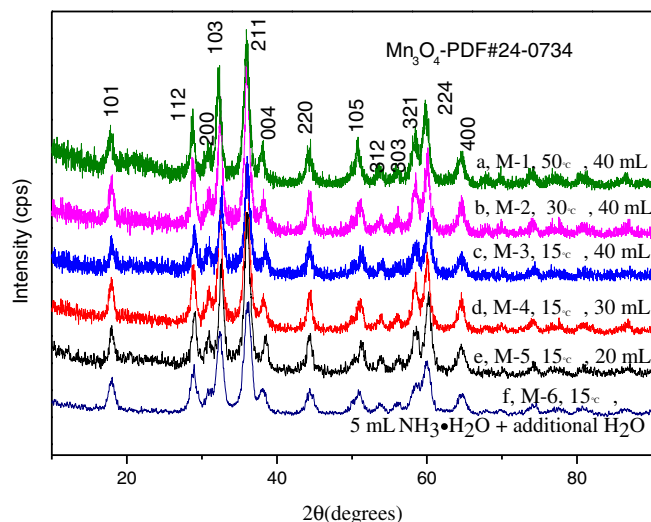
2.4 *Measurements*

Crystal structures of the as-synthesized Mn$_3$O$_4$ and LiMn$_2$O$_4$ materials were analysed by a X-ray diffraction (XRD, Rigaku, D/Max-2400) measurement with Cu–Kα radiation (40 kV, 150 mA, step size = 0.02°.s^{-1}), respectively. The morphologies were observed on a transmission electron microscopy (TEM, FEI Tecnai G2 F20) and a scanning electronic microscopy (SEM, Hitachi, S-4800) for Mn$_3$O$_4$ and LiMn$_2$O$_4$ materials, respectively. Electrochemical properties tests of cells were carried out on a land cell tester CT2001A (Wuhan, China) in the voltage range of 3.5–4.3 V at room temperature.

3. Results and discussion

3.1 *Characterization of Mn₃O₄ materials*

The XRD analysis of the as-synthesized Mn$_3$O$_4$ nanoparticles was carried out, as shown in figure 1a. The planes corresponding to (101), (112), (220), (103), (211), (004), (220), (105), (312), (303), (321), (224), (400) and (305) are in good agreement with the standard values of tetragonal hausmannite Mn$_3$O$_4$ structure (JCPDS NO. 24-0734).[18] No additional peaks of other phases have been detected, indicating high purity and good crystallinity of the Mn$_3$O$_4$ products. Mn$_3$O$_4$ is well-known to have the normal spinel structure in which the Mn^{2+} ions occupy the tetrahedral sites while the Mn^{3+} ions occupy the octahedral sites. Mn$_3$O$_4$ also has a stable tetrahedral structure in which the oxygen octahedron is tetragonally distorted due to the Jahn–Teller effect on Mn^{3+} ions.[19]

The corresponding morphology of the as-synthesized Mn$_3$O$_4$ nanoparticles was observed by TEM analysis, as shown in figure 2a$_1$ and b$_1$. From TEM images, it can be seen that Mn$_3$O$_4$ nanoparticles are square-shaped with the side length of about 4.5 nm. A typical selected-area electron diffraction (SAED) pattern (figure 2c for M-1) confirms that the nanoparticles are nano-sized Mn$_3$O$_4$ crystals.
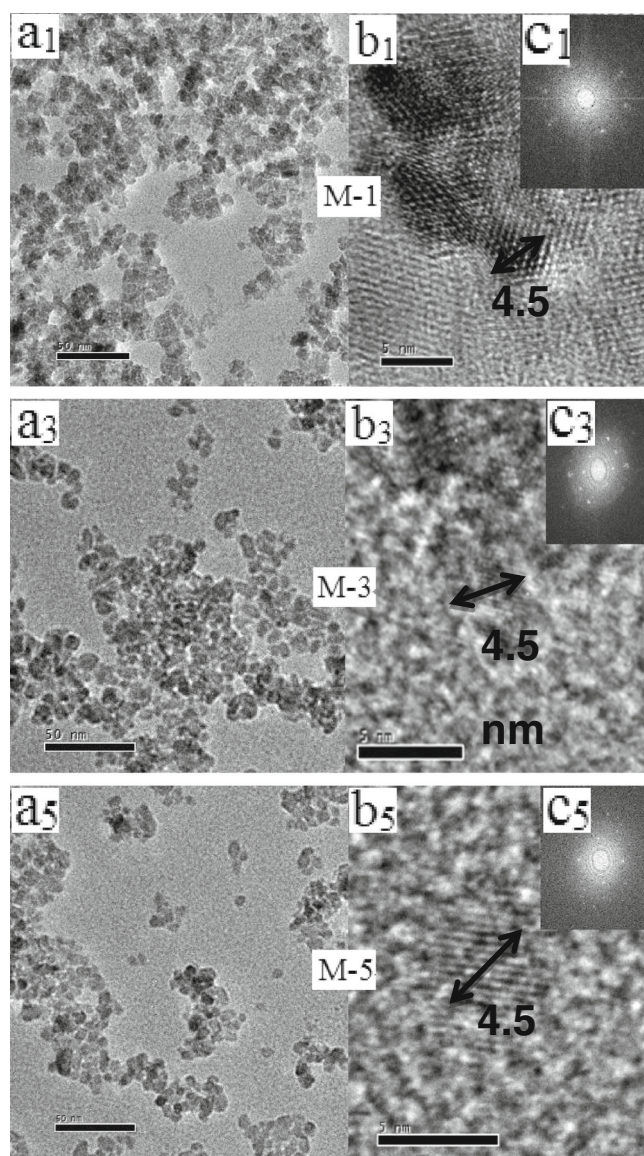
Figure 2. (**a**) Low-resolution TEM images, (**b**) high-resolution TEM images and (**c**) the typical SAED patterns of the as-synthesized Mn$_3$O$_4$ nanoparticles.

Figure 1. XRD patterns of the samples of Mn$_3$O$_4$ materials using different amount of NH$_3$·H$_2$O at different temperatures.

3.2 *The rapid preparation mechanism of nano-sized Mn_3O_4 crystals*

It takes only 5 min to prepare nano-sized Mn_3O_4 crystals by a gas–liquid reaction method. The rapid preparation mainly benefits from replacing a gas–solid reaction with a gas–liquid reaction. Different from the existence of $Mn(OH)_2$ precipitates under alkaline condition, nano-sized Mn_3O_4 crystals could be obtained via the reaction between O_2 and soluble Mn(II) coordination complexes.

In order to effectively study the form of Mn(II) coordination complexes existing in the solution, many supporting experiments were carried out. Details, results and discussion are as follows:

(i) All other things being equal, $Mn(OH)_2$ precipitates would be formed when the solvent of ethanol was replaced by water. And hardly any manganese compounds could be detected in the solution after filtration. It indicates that the solvent of ethanol is involved in Mn(II) coordination complexes, or the resulting soluble Mn(II) coordination complexes are unstable in a larger amount of water.

(ii) All other things being equal, $Mn(OH)_2$ precipitates would be formed when the $NH_3 \cdot H_2O$ was replaced by a NaOH solution with the same pH. And hardly any manganese compounds could be detected in the solution after filtration. It indicates that the addition of $NH_3 \cdot H_2O$ materials provides not only the alkaline condition for the oxidation of Mn(II), but also NH_3 molecules as ligands.

(iii) All other things being equal, $Mn(OH)_2$ precipitates would be formed when $Mn(CH_3COO)_2$ materials were replaced by $MnCl_2$ and $Mn(NO_3)_2$ materials, respectively. But with the addition of sufficient concentrations of certain acetate compounds (CH_3COONH_4, for example), $Mn(OH)_2$ precipitates would disappear, and the solution containing Mn(II) coordination complexes would be obtained again. It indicates that CH_3COO^- anions play an important role in the formation of stable Mn(II) coordination complexes.

(iv) All other things being equal, no $Mn(OH)_2$ precipitates was formed when $Mn(CH_3COO)_2$ materials were replaced by a mixture of $MnCl_2$ and $Mn(CH_3COO)_2$ materials, with the molar ratio of 4:5 or less. But when the molar ratio was more than 4:5, part of $Mn(OH)_2$ precipitates would be formed to consume the relatively excessive Mn(II) ions, and keep a 9:10 molar ratio of soluble Mn(II) ions to CH_3COO^- anions in solution. It suggests that CH_3COO^- anions are taken part in coordination with the complex ratio of 9:10 for Mn(II) ions to CH_3COO^- anions.
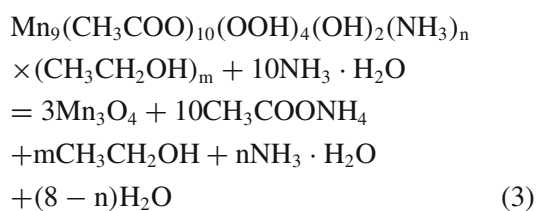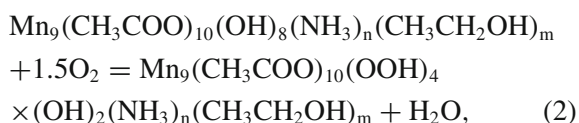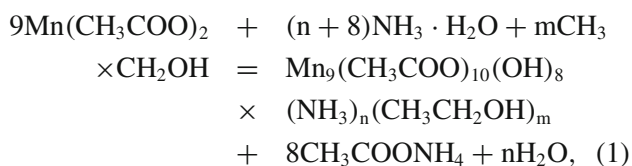
(v) All other things being equal, nano-sized Mn_3O_4 crystals, which have been characterized by XRD analysis (figure 1b–e), could also been prepared using different amounts of $NH_3 \cdot H_2O$ at different temperatures, as shown in table 2. It could be seen that the preparation time is increased with decrease in the temperature and the increase of usage amounts of $NH_3 \cdot H_2O$. Besides, as representative samples, M-3 and M-5 were observed by TEM analysis, as shown in figures 2 (a_3, b_3) and (a_5 and b_5). Small particals got from every method are square-shaped with the side length of about 4.5 nm. That is to say, the morphology and size of nano-sized Mn_3O_4 crystals are free from the effect of temperature and usage amounts of $NH_3 \cdot H_2O$.

(vi) All other things being equal, with the temperature being lowered to 15°C as well as the raw materials of $NH_3 \cdot H_2O$ (25 wt%–28 wt%) being decreased to 5 mL, a deep black solution would be got with 30 min of oxidation process. The resulting black solution could stay stable more than 12 h, without any suspended solid. The average oxidation state of Mn coordination complexes was measured to be 2.67, which was equal to the oxidation state in Mn_3O_4 materials. And when enough water was added into the black solution, black suspended solids were produced immediately. Removing the supernatant after centrifugation, small particles named M-6 were obtained. The XRD analysis of the as-synthesized M-6 was carried out, as shown in figure 1f. All diffraction peaks can be perfectly indexed to the Mn_3O_4 structure (JCPDS NO. 24-0734). It suggests that part of Mn(II) coordination complexes are oxidized, consequently forming Mn(III)Mn(III)Mn(II) coordination complexes in solution. Based upon these results, we can conclude that the resulting Mn(III)Mn(III)Mn(II) coordination complexes is stable with relatively low concentration of water (brought by the raw materials of $NH_3 \cdot H_2O$). But, when the concentration of water is high, Mn(III)Mn(III)Mn(II) coordination complexes will decompose immediately to form nano-sized Mn_3O_4 crystals. These deductions are supported form table 2, which shows that the preparation time is increased with the decrease of $NH_3 \cdot H_2O$. In addition, a possible conclusion is that rate-determining step for the preparation of nano-sized Mn_3O_4 crystals is the oxidation process from Mn(II) coordination

Table 2. Preparation details of nano-sized Mn$_3$O$_4$ crystals using different amounts of NH$_3$·H$_2$O at different temperatures.
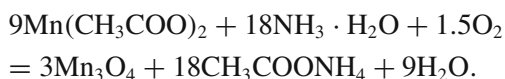
Material code	Temperature (°C)	Usage amounts of NH$_3$·H$_2$O (mL)	Preparation time (min)
M-2	30	40	10
M-3	15	40	25
M-4	15	30	37
M-5	15	20	65

complexes to Mn(III)Mn(III)Mn(II) coordination complexes.

Coupled with these supporting experiments in literatures,[20,21] the chemical reaction equations maybe as follows:

$$9Mn(CH_3COO)_2 + (n+8)NH_3 \cdot H_2O + mCH_3$$
$$\times CH_2OH = Mn_9(CH_3COO)_{10}(OH)_8$$
$$\times (NH_3)_n(CH_3CH_2OH)_m$$
$$+ 8CH_3COONH_4 + nH_2O, \quad (1)$$

$$Mn_9(CH_3COO)_{10}(OH)_8(NH_3)_n(CH_3CH_2OH)_m$$
$$+1.5O_2 = Mn_9(CH_3COO)_{10}(OOH)_4$$
$$\times (OH)_2(NH_3)_n(CH_3CH_2OH)_m + H_2O, \quad (2)$$

$$Mn_9(CH_3COO)_{10}(OOH)_4(OH)_2(NH_3)_n$$
$$\times (CH_3CH_2OH)_m + 10NH_3 \cdot H_2O$$
$$= 3Mn_3O_4 + 10CH_3COONH_4$$
$$+mCH_3CH_2OH + nNH_3 \cdot H_2O$$
$$+(8-n)H_2O \quad (3)$$

And the overall reaction is:

$$9Mn(CH_3COO)_2 + 18NH_3 \cdot H_2O + 1.5O_2$$
$$= 3Mn_3O_4 + 18CH_3COONH_4 + 9H_2O.$$

Though the preparation mechanism is not exactly clear, the rapid production method for making nano-sized Mn$_3$O$_4$ crystals is of great significance to reduce costs. And better yet, both Mn(II) and Mn(III)Mn(III)Mn(II) coordination complexes are prepared in ammonia alkaline solutions with simple methods. That is constructive not only to accelerate reaction rates for similar preparations, but also to inspire interest in similar coordination complexes containing nickel ions and cobalt ions.
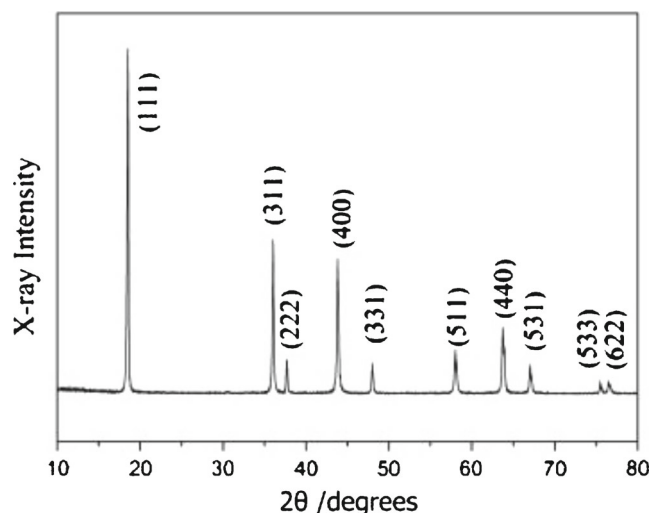
3.3 *Characterization of LiMn$_2$O$_4$ materials*

As an extension of the synthesis of nano-sized Mn$_3$O$_4$ crystals, the intermediate ammonia alkaline solution containing Mn(III)Mn(III)Mn(II) coordination complexes are used to prepare nano-sized LiMn$_2$O$_4$ materials. Due to the fact that Mn(III)Mn(III)Mn(II) coordination complexes trend to decompose into nano-sized Mn$_3$O$_4$ crystals spontaneously, the newly as-synthesized nano-sized Mn$_3$O$_4$ crystals could be dispersed evenly and stable throughout the liquid. That is good for the precise control of the stoichiometric amount at the micro level for Mn$_3$O$_4$ and Li$^+$ ions.

The XRD analysis of the as-synthesized LiMn$_2$O$_4$ nanoparticles was carried out, as shown in figure 3. All diffraction peaks can be perfectly indexed to the LiMn$_2$O$_4$ structure (JCPDS NO. 35-0782). The result indicates that high-purity and well-crystallized LiMn$_2$O$_4$ materials could be obtained via the novel method, taking advantages of the elevated oxidation state of manganese ions and the precise control of the stoichiometric amount for raw materials at the micro level.

Figure 4 shows SEM and TEM analysis of LiMn$_2$O$_4$ nanoparticles. Although any physical treatment has been done to disperse powders, the as-synthesized LiMn$_2$O$_4$ nanoparticles are still present with homogeneous size distribution without any obvious agglomeration. Besides, the average particle size is about

Figure 3. The XRD pattern of LiMn$_2$O$_4$ materials.

24.2 nm, estimated from relative TEM images using Nano Measurer version 1.2.5, by manually selecting 50 particles. As shown in the illustration of figure 4b, the particle size distribution is concentrated at 21.7–29.5 nm (90.8% of the total), particularly at 21.7–25.6 nm (62.0% of the total). Both of the good dispersibility and the small particle size are benefited greatly from the intermediate nano-sized Mn_3O_4 crystals and are the preferred sol–gel preparation method. Firstly, nano-sized Mn_3O_4 crystals provide plenty of nucleation sites to form nano-sized $LiMn_2O_4$ structures. Secondly, the preferred sol–gel method, which has been recognized as a new practical technology to prepare the nanometer-sized catalysts, could homogeneously mix Mn(III)Mn(III)Mn(II) coordination complexes (with consequent decomposition to form a colloidal solution containing nano-sized Mn_3O_4 crystals) with $LiNO_3$ at a micro level. Thirdly, both of the similar crystal structure of Mn_3O_4 to $LiMn_2O_4$ and the
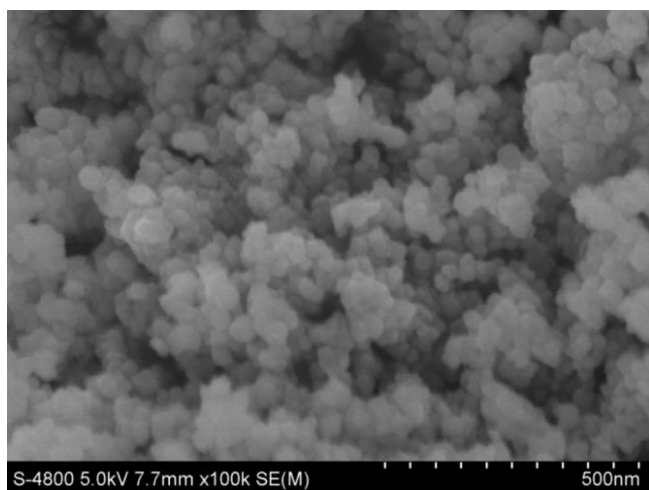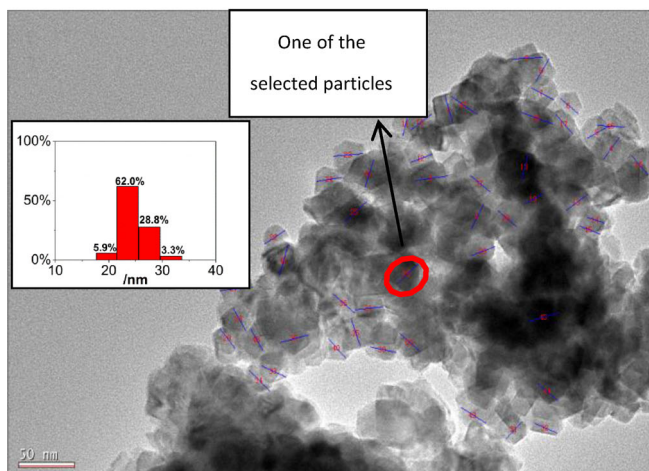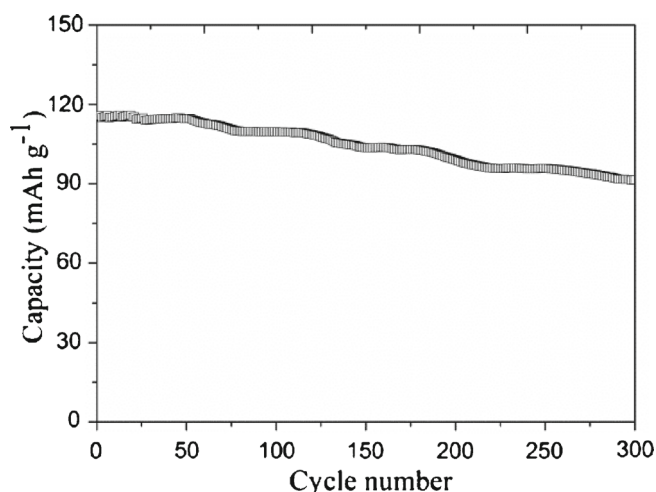

Figure 4. (**a**) SEM and (**b**) TEM images of $LiMn_2O_4$ materials.

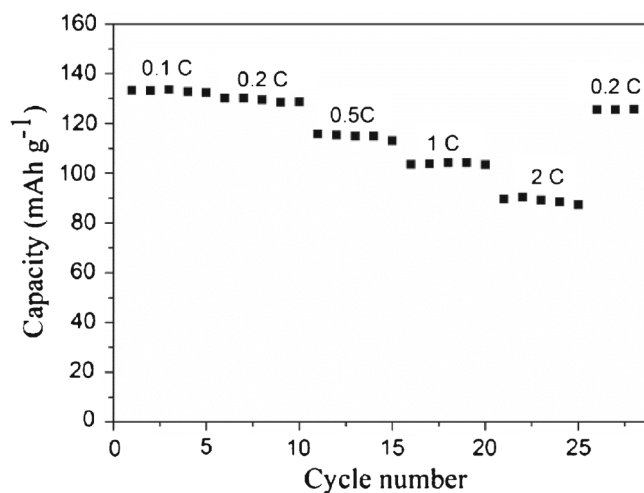**Figure 5.** The cycle performance for $LiMn_2O_4$/Li cell with 0.5 C of discharge rate at room temperature.

homogeneous mixture of all reagents are good for the formation of dispersed nano-sized $LiMn_2O_4$ at low temperature (at 650°C, for example).

3.4 *Electrochemical properties of LiMn₂O₄/Li half cells*

To study the electrochemical properties of the nano-sized $LiMn_2O_4$ materials prepared by the novel method, $LiMn_2O_4$/Li half cells were assembled and tested. Figure 5 shows the cycle performance of $LiMn_2O_4$/Li cells with 0.5 C of discharge rate at room temperature. $LiMn_2O_4$ nanoparticles shows good cycle performance which initially delivers 115.4 mAh·g^{-1} and retains 91.4 mAh·g^{-1} (79.2%) at the 300th cycle.

Figure 6. Cycle performances of $LiMn_2O_4$/Li cells with different discharge rates at room temperature.

The discharge capacities of $LiMn_2O_4$/Li cells with different discharge rates at room temperature are shown in figure 6. The nanoscale materials which could bring not only both high surface area and the short diffusion distance during the charge–discharge process, but also improve the rate capability of every cell with the discharge capacities of 133 mAh·g^{-1} and 90 mAh·g^{-1} at rates of 0.1 C and 2 C, respectively.[22,23]

4. Conclusion

A facile method has been successfully developed for the synthesis of nano-sized Mn_3O_4 crystals. By replacing the most common gas–solid reaction with a novel gas–liquid reaction, 4.5 nm of Mn_3O_4 crystals are prepared in redox reactions in 5 min at 50°C.

Besides, as the extension of synthesis of nano-sized Mn_3O_4 crystals, the intermediate ammonia-alkaline solution containing Mn(III)Mn(III)Mn(II) coordination complexes, which tend to decompose into nano-sized Mn_3O_4 crystals spontaneously, are used to prepare nano-sized $LiMn_2O_4$ materials. Due to the fact that the as-synthesized nano-sized Mn_3O_4 crystals could be dispersed evenly and stable in the solution, this method is good for the precise control of the stoichiometric amount at the micro level for Mn_3O_4 and Li$^+$ ions. The novel method is constructive not only to accelerate reaction rates for the elevated oxidation state of manganese ions, but also to prepare dispersed nano-sized $LiMn_2O_4$ materials with good electrochemical properties.

References

1. Piligkos S, Rajaraman G, Soler M, Kirchner N, Van Slageren J, Bircher R, Parsons S, Gudel H U, Kortus J, Wernsdorfer W, Christou G and Brechin E K 2005 *J. Am. Chem. Soc.* **127** 5572
2. Yoshikai N, Zhang S L, Yamagata K I, Tsuji H and Nakamura E 2009 *J. Am. Chem. Soc.* **131** 4099
3. Reddy A L M, Shaijumon M M, Gowda S R and Ajayan P M 2009 *Nano Lett.* **9** 1002
4. Kolts J H and Delzer G A 1986 *Science* **232** 744
5. Li X Q, Zhou L P, Gao J, Miao H, Zhang H and Xu J 2009 *Powder Technol.* **190** 324
6. Zhang L C, Zho Q U, Liu Z H, Hou X D, Li Y B and Lv Y 2009 *Chem. Mater.* **21** 5066
7. Zhang H M, Lian C H G, Tian Z F, Wang G Z and Cai W P 2010 *J. Phys. Chem. C* **114** 12524
8. Durmus Z, Baykal A, Kavas H, Direkci M and Toprak M S 2009 *Polyhedron* **28** 2119
9. Davar F, Salavati-Niasari M, Mir N, Saberyan K, Monemzadeh M and Ahmadi E 2010 *Polyhedron* **29** 1747
10. Mehdizadeh R, Saghatforoush L A and Sanati S 2012 *Superlattice Microst.* **52** 92
11. Anilkumar M and Ravi V 2005 *Mater. Res. Bull.* **40** 605
12. Fang Z, Tang K, Gao L, Wang D, Zeng S and Liu Q 2007 *Mater. Res. Bull.* **42** 1761
13. Wang N, Guo L, He L, Ca X O, Chen C P, Wang R and Yang S H 2007 *Small* **3** 606
14. Hu G R, Jiang J B, Pen Z D G, Du K, Cao Y B and Duan J G 2013 *J. Nanosci. Nanotechnol.* **13** 2262
15. Lu Z Y, Rui X H, Tan H T, Zhang W Y, Hng H H and Yan Q Y 2013 *Chem. Plus. Chem.* **78** 218
16. Xiang X D, Fu Z and Li W S 2013 *J. Solid State Electrochem.* **17** 1201
17. Ni L P, Cheng X M, Wang X F, Tao Y L, Shen Y H, Zhang T, Sun H R and Xie A J 2013 *Ionics* **19** 259
18. Liu L, Yang H X, Wei J J and Yang Y Z 2011 *Mater. Lett.* **65** 694
19. Dubal D P and Holze R 2012 *RSC Adv.* **2** 12096
20. Christmas C, Vincent J B, Chang H R, Huffman J C, Christou G and Hendrickson D N 1988 *J. Am. Chem. Soc.* **110** 823
21. Hu C C, Wu Y T and Chang K H 2008 *Chem. Mater.* **20** 2890
22. Jo M, Lee Y K, Kim K M and Cho J 2010 *J. Electrochem. Soc.* **157** 841
23. Cui X L, Li Y L, Li S Y, Li L X and Liu J L 2013 *Ionics* **19** 1489